LOS ALAMOS SCIENTIFIC LABORATORY

of

THE UNIVERSITY OF CALIFORNIA

May 1, 1951

VERIFIED UNCLASSIFIED

EMS   JUN 1 5 1979

LA-1251

This document consists of __47__ pages

No. __20__ of __20__ copies, Series A.

CRITICAL MASSES OF ORALLOY AT
REDUCED CONCENTRATIONS AND DENSITIES

Work done by:

Members of Group W-2

Report written by:

I-II: J. D. Orndoff
III : H. C. Paxton
IV : G. E. Hansen

WEAPON DATA

ABSTRACT

From Pajarito measurements on Oy cores of various densities and concentrations in an 8" thick Tu tamper, relations between critical mass and Oy density and concentration are obtained. The Oy critical mass is approximately proportional to $\rho^{-1.2}c^{-1.7}$ for densities ranging from 50% to 100% of normal and 25 concentrations from 47% to 94%. Results are compared with predictions based on current values of 25 and 28 cross sections.

TABLE OF CONTENTS

CRITICAL MASSES OF ORALLOY AT
REDUCED CONCENTRATIONS AND DENSITIES

I. INTRODUCTION

The following equation has been used almost universally in the past to predict the variation of critical masses with density and concentration of a tuballoy-tamped oralloy core:

$$M_c = \text{const } \rho_c^{-1.4} \rho_t^{-.6} c^{-1.8} \tag{1}$$

where ρ_c = density of core;

ρ_t = density of tamper;

c = concentration of core.

The origin of the above expression is rather obscure. It certainly dates back to early days as it appears explicitly in the handbook supplement, LA-140A. Relationships between critical radius and mean free paths published in T-Division Progress Reports for 1944 (e.g. LAMS-123, page 11) are sufficient to deduce the density dependence. Theoretical work by Serber's group found that critical mass should vary as $\rho_t^{-.6}$ and simple considerations show that the sum of the exponents on core density and tamper density must equal -2.

In Chapter 1 of LA-1028, Vol. VI of the Los Alamos Technical Series, Weisskopf states (without further discussion): "If only the core density is changed, the critical mass changes with a power less than the second. Theory shows that it is the

- 5 -

1.2 power of the density change."

In discussions of the apparent variability of the core density exponent, it has been suggested that the value 1.2 refers to a static system, and that 1.4 refers to a highly supercritical system where time absorption in the tamper makes tamper compression of less relative importance.

A concentration relation can be obtained from Fig. 2 of LA 235, which is a curve of critical mass of 25 for a WC tamper. When these data are plotted on log-log paper, a perfect $c^{-1.8}$ dependence is observed.

It can be seen that the density-concentration relation is semi-empirical as it was deduced by getting the best fit with theoretical calculations based on core and tamper properties. The relation first appeared in 1944 and consequently a recalculation using presently revised core and tamper constants might yield a somewhat different power relation.

The purpose of the following report is to establish as firmly as possible a concentration-density law on the basis of (a) critical mass and replacement measurements on low concentration and low density assemblies; and (b) theoretical considerations using presently known core and tamper constants.

II.   CRITICAL MASS MEASUREMENTS

A.   Apparatus

Topsy, a remotely controlled assembly machine at Pajarito Site, was used for the experiments (see Fig. 1). The effectively infinite (8 to 8½ inches thick) tuballoy tamper is shown on the platform at the right. The active material was stacked inside the tuballoy can on the cart. The remote operations consisted of moving the cart to the right underneath the tamper platform and then raising the can by means of a hydraulic piston until the active material was assembled in the tamper.

Active material was in the form of oralloy blocks. Three sizes were available: ½ inch cubes, ½ x ½ x 1 inch blocks, and 1 x 1 x ½ inch blocks. All core assemblies were in the form of pseudospheres which (excepting an intentional deviation) were made as symmetric as possible and were stacked entirely on the ram. Low concentration pseudospheres were stacked by using Oy and Tu blocks in the correct proportions. Low densities were realized by leaving appropriately spaced ½ x ½ x ½ inch "voids" throughout the pseudospheres. These voids were produced by using spacers made of ½ inch diameter, ½ inch long, 1/16 inch wall aluminum cylinders. The amount of aluminum involved was thus kept quite low. An example of the pseudosphere type of stacking in the ram is shown in Fig. 2. The stacking in the picture was
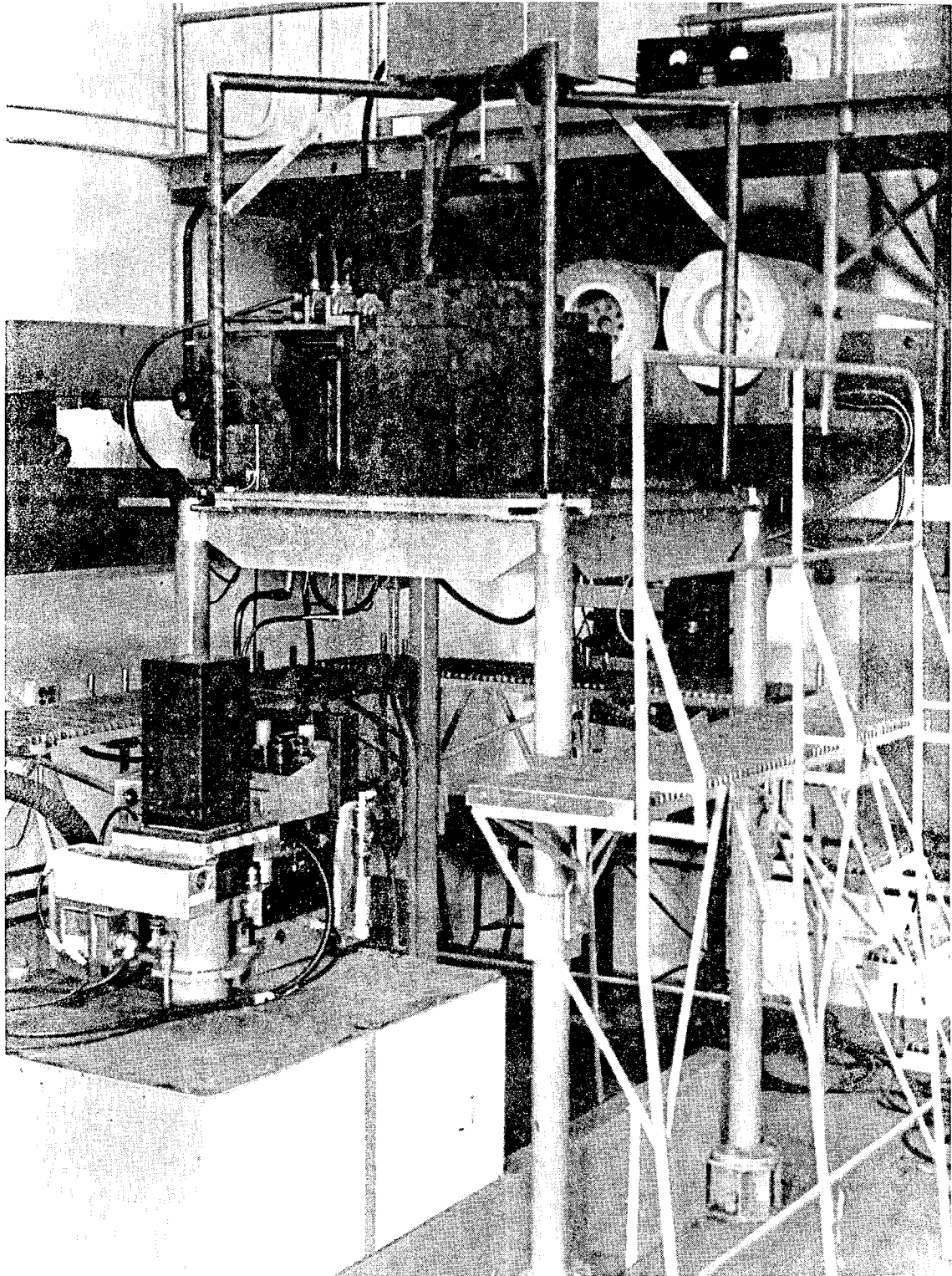
FIG. 1.   Topsy, the universal machine for assembling
critical configurations.
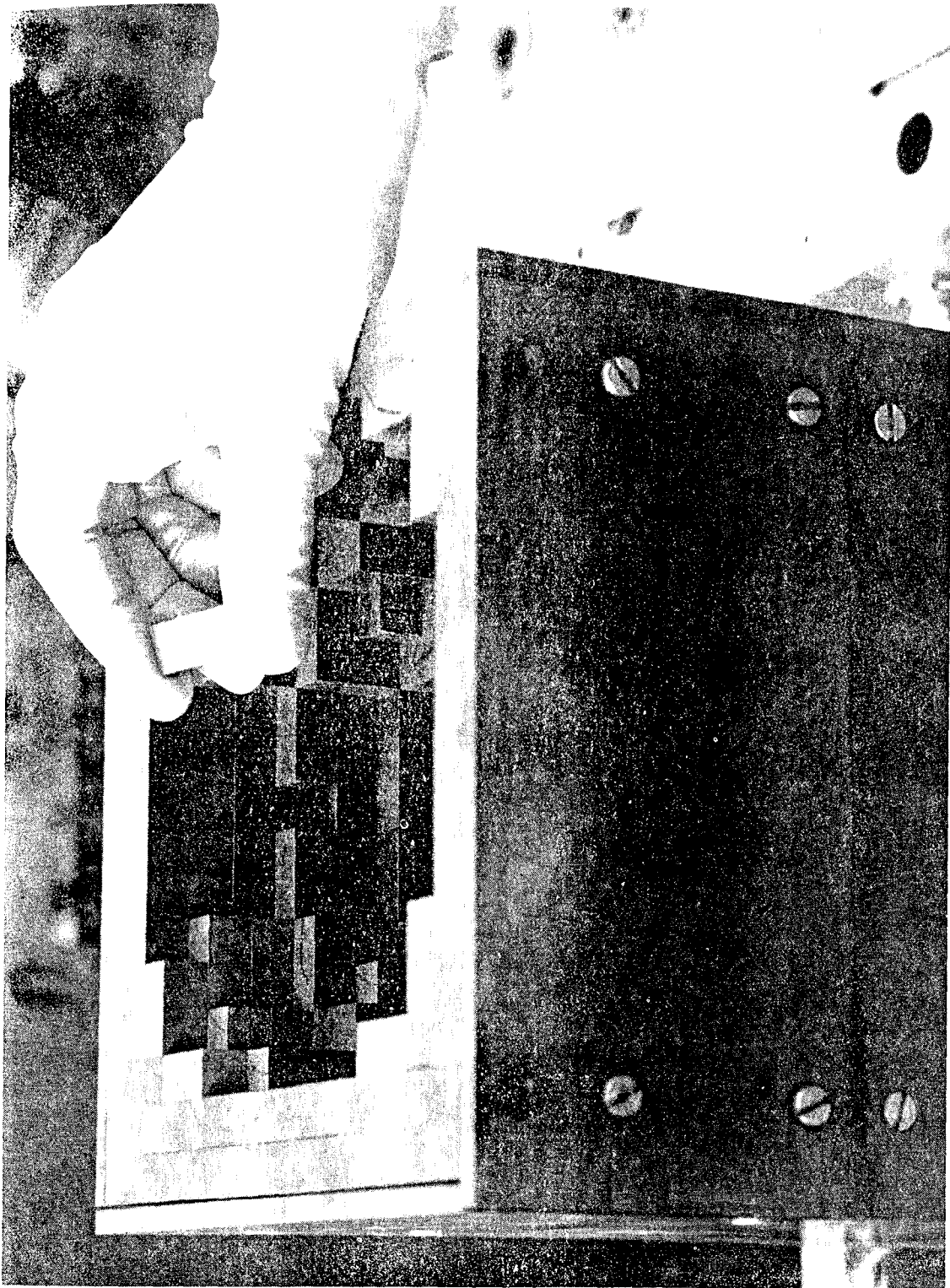
FIG. 2.   Oralloy being stacked into cavity in Topsy ram.

for another experiment where half of the active material was on the ram and half supported in the tamper, but the figure illustrates the general procedures.

The critical condition was approached in each case by making central source multiplication measurements as increments of active material were added to complete a pseudosphere. Curves of reciprocal multiplication vs mass of active material were plotted up to multiplications of approximately 100. The source was then moved to an external position and the assembly stacked on up to critical. Thus, for each different density or concentration configuration, the exact critical mass was determined without extrapolation.

B.   Low Concentration Experiments

The starting point of all the measurements was the determination of the critical mass of normal density and concentration oralloy. This was done very carefully, and the weight and concentration of every piece of oralloy in the assembly was recorded. These data, along with some other pertinent data, are tabulated in Table I.

Low concentration pseudospheres were obtained by "diluting" with ½ x ½ x ½ inch units of tuballoy to give configurations with 85%, 70% and 50% oralloy. Since normal oralloy concentration was 94%, the resultant average U^{235} concentra-

tions were 80%, 66% and 47%. The distribution of tuballoy cubes in all cases was made as uniform as possible. Every layer was stacked to have very nearly the same concentration as the average for the whole pseudosphere. Also successive layers were arranged so that tuballoy cubes did not superimpose. Stacking diagrams for the low concentration pseudospheres are given in Figs. 3, 4, 5 and 6. The experimental results are summarized in Table II.

TABLE I.   Standard stacking information.

Critical mass- -	17.41 kg
Average concentration- - - - - - - - - - - - - - - - - -	94.13%
Range of concentration - - - - - - - - - - - - - -	93.6 to 95.4%
Average density- - - - - - - - - - - - - - - - - -	18.72 gm/cm^3
Average weight of ½" Oy cube - - - - - - - - - - - -	38.35 gm
Average weight of ½" Tu cube - - - - - - - - - - - - -	38.57 gm
Tamper thickness -	8½" Tu

■ Al Spacer

☐ Oy Cube
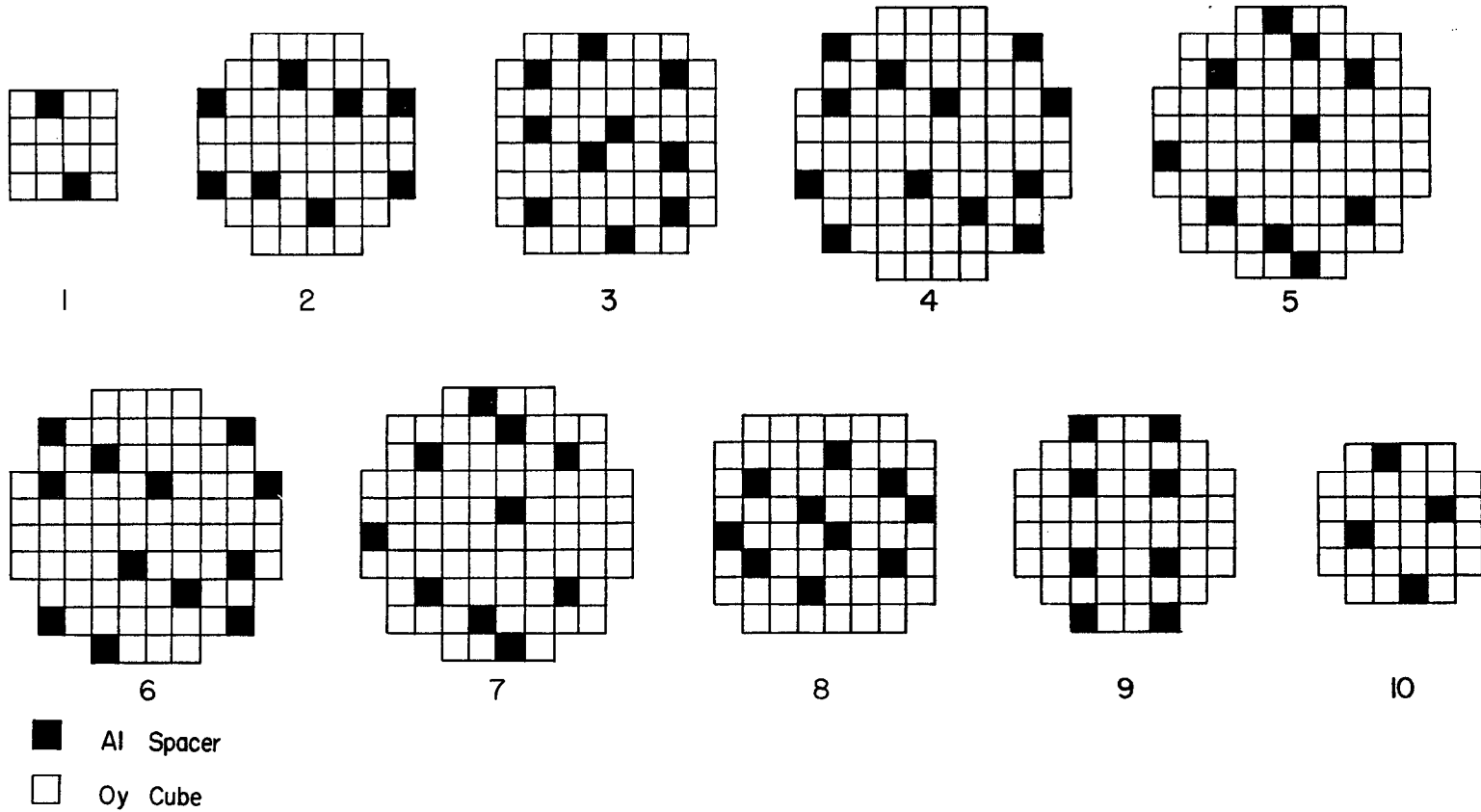
FIG. 3.   Stacking diagram for 5" pseudosphere; 85% stacking concentration; 80.5% actual concentration.

LAYER 1   LAYER 2   LAYER 3   LAYER 4   LAYER 5   LAYER 6

LAYER 7   LAYER 8   LAYER 9   LAYER 10   LAYER 11

■ Tu cube
□ Oy cube
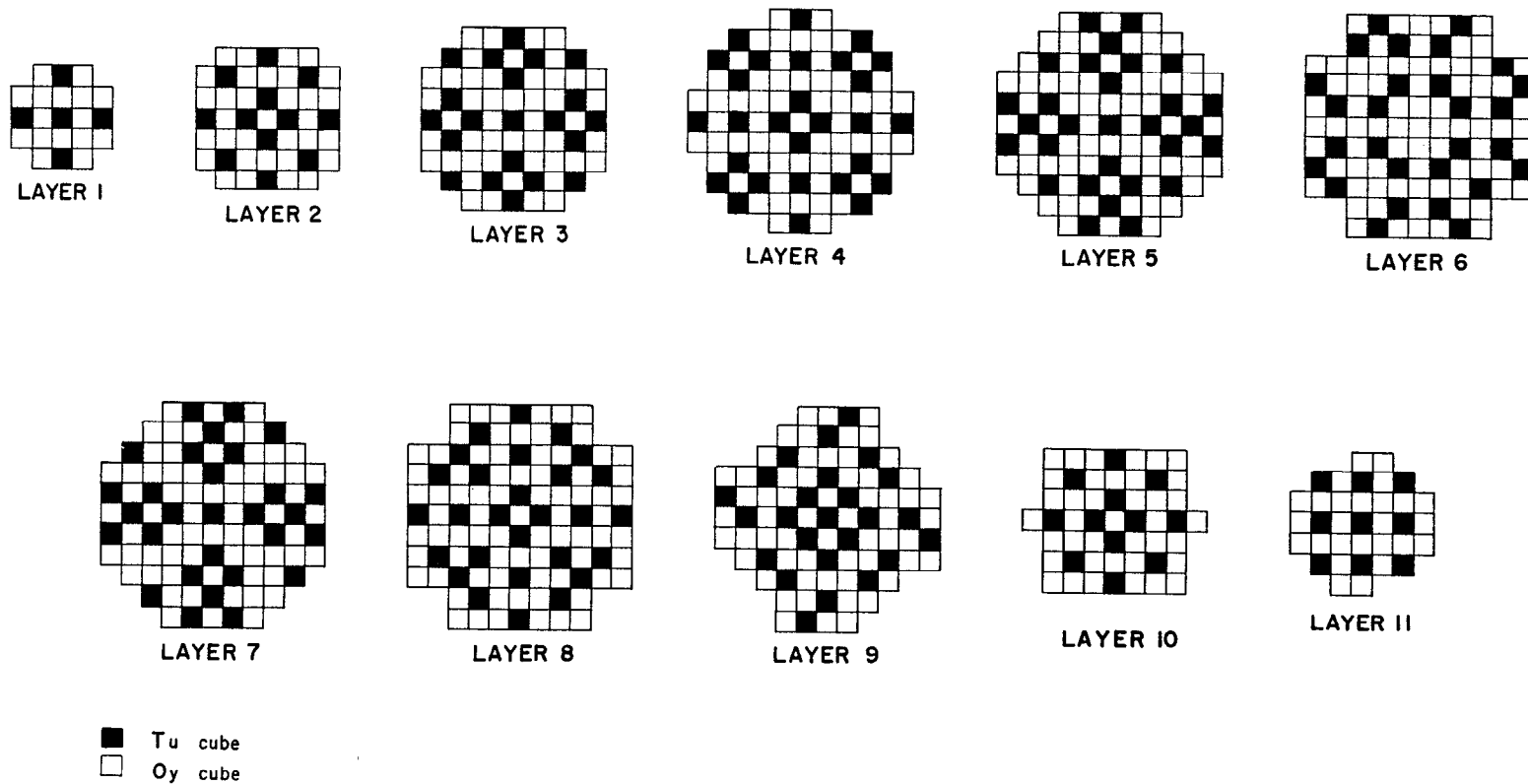
FIG. 4.   Stacking diagram for 5½" pseudosphere; 70% stacking concentration; 67.6% actual concentration.
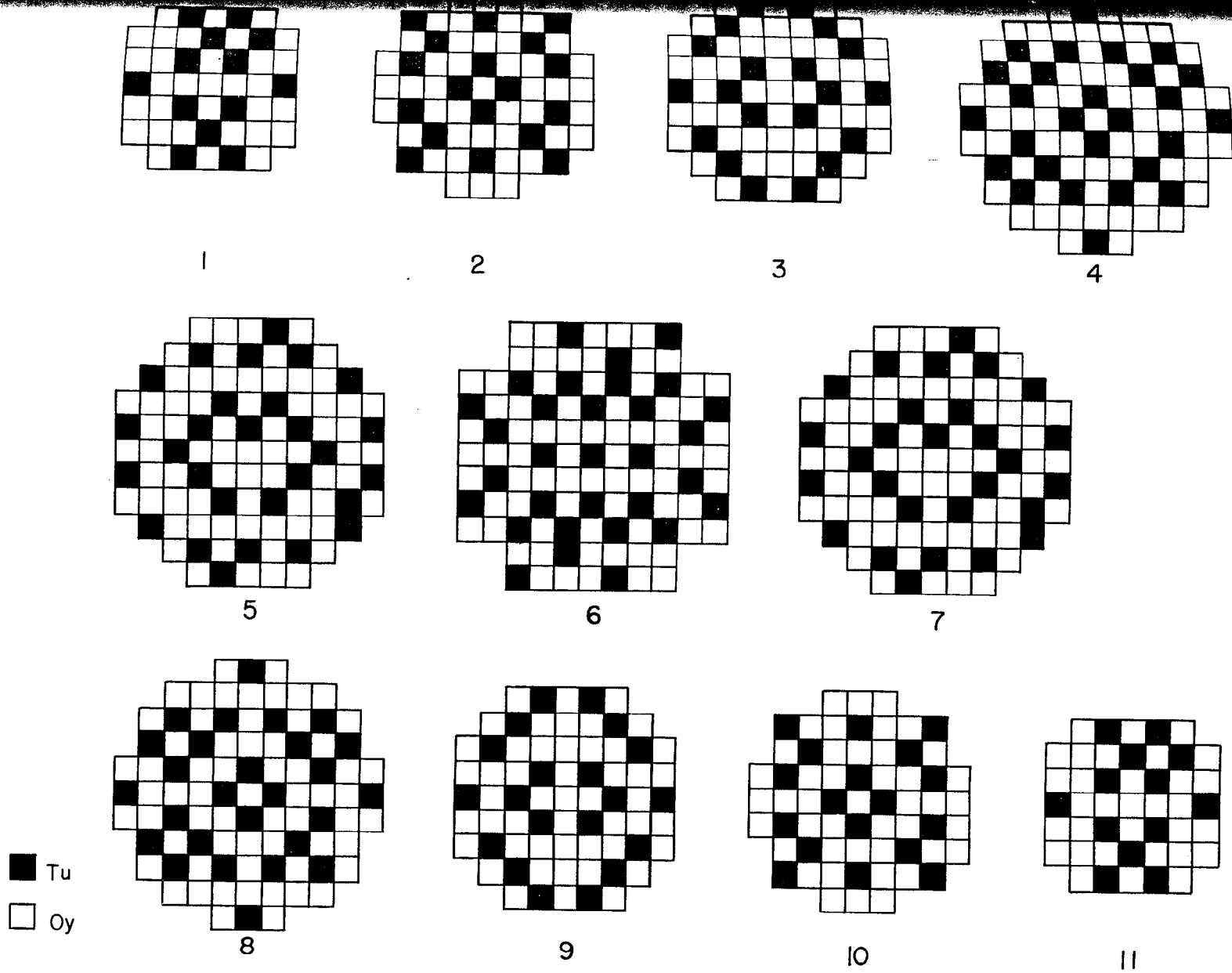
FIG. 5. Stacking diagram for 5½" pseudosphere; 70% stacking concentration; 66.6% actual concentration.

■ Tu

□ Oy
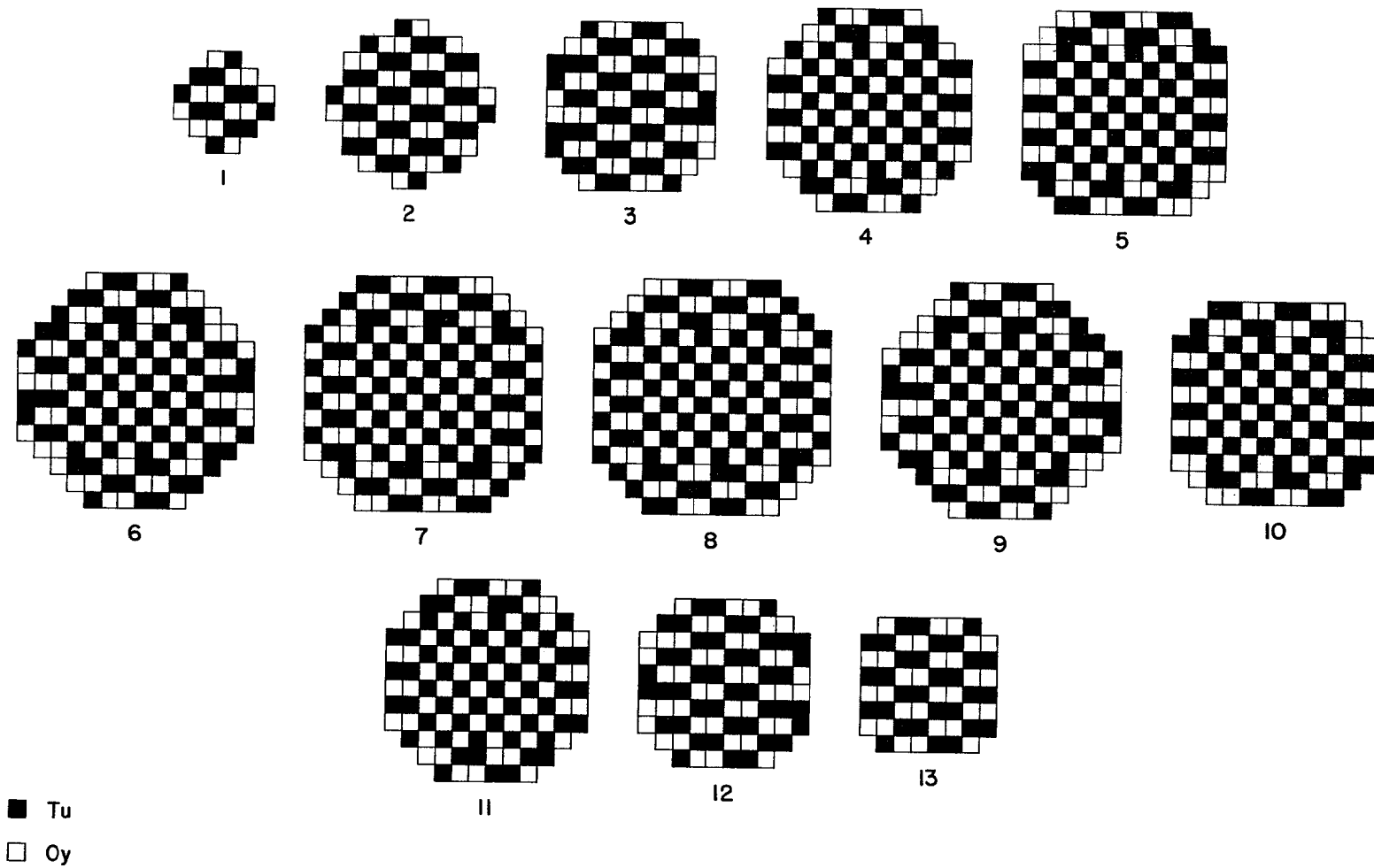
FIG. 6. Stacking diagram for 7" pseudosphere; 50% stacking concentration; 47.3% actual concentration.

TABLE II. Critical mass vs core concentration for oralloy-tuballoy assembly.

Percent concentration	Pseudosphere size (in)	M_c (kg)	No.units Oy	No.units Tu	Oy weight (kg)	Tu weight (kg)	Concentration exponent
94.13	4.5	17.41	454	0	17.41	0	
80.5	5	22.73	506	86	19.41	3.32	1.70
67.6	5.5	30.73	574	226	22.01	8.72	1.72
66.6	5.5	31.84	586	243	22.47	9.37	1.75
47.3	7	57.23	744	744	28.53	28.70	1.73

There was some concern that even though the average con-
centration of each layer was correct, there might be consi-
derable variation of concentration radially. This was checked
by investigating the structure of the central 2 inch cube for
both the low concentration and low density cases. Considera-
ble variation from average density and concentration was
found in several cases and, since this central material would
have a larger effect on criticality than outside material, it
was decided to make a check to find out how much error could
arise from this source. The 67.6% concentration stacking was
found to be the worst. As the central 2 inch cube had an av-
erage concentration of 73%, a second stacking diagram was made
corresponding to 66.6% concentration. Great care was taken to
have the central region with the correct average concentration.
The more precise stacking changed the concentration exponent
from 1.72 to 1.75. Since the total variation in this extreme
case was less than 2%, it was concluded that the other stack-
ings were satisfactory.

C. Low Density Experiments

Low density critical mass measurements were made by leav-
ing appropriately spaced ½ x ½ x ½ inch voids throughout the
assembly to average 85%, 70%, and 50% of normal density. In
order to support Oy cubes over the void positions, it was neces-

sary to insert cylindrical aluminum spacers. The experiment
was then complicated by the fact that corrections had to be
made for the presence of aluminum in the assemblies. These
corrections were determined by making two stackings at the
same density with quantities of aluminum differing by approxi-
mately a factor of two. The mass of aluminum was doubled by
dropping aluminum slugs inside the hollow cylindrical spacers.
The critical masses were then extrapolated to zero aluminum by
assuming that the reactivity change due to aluminum varies li-
nearly with its mass. Stacking diagrams for the low density
pseudospheres are given in Figs. 7, 8, 9 and 10. Stacking dia-
grams are included only for the case of aluminum spacers with-
out slugs. The stackings for doubled aluminum were identical
except that critical was reached at slightly lower masses in
each case. The experimental results are listed in Table III.

Two 85% stackings were made. The 5.5 inch pseudosphere
was deliberately made non-symmetrical. Three layers were miss-
ing at critical so that one "diameter" was only four inches.
The symmetry here was much worse than any other pseudosphere,
yet the density exponent was not out of line with the other
determinations. It can be assumed then that any errors due to
shape factor are negligible. There was no direct measurement
made of the effect of aluminum in the case of 85% density.
Since the mass of aluminum in this case was small, the correc-
tion was estimated by considering the effect of aluminum in
the 70% and 50% density stackings.

1   2   3   4   5

6   7   8   9A

◼ Al Spacer

◻ Oy Cube

9B   10
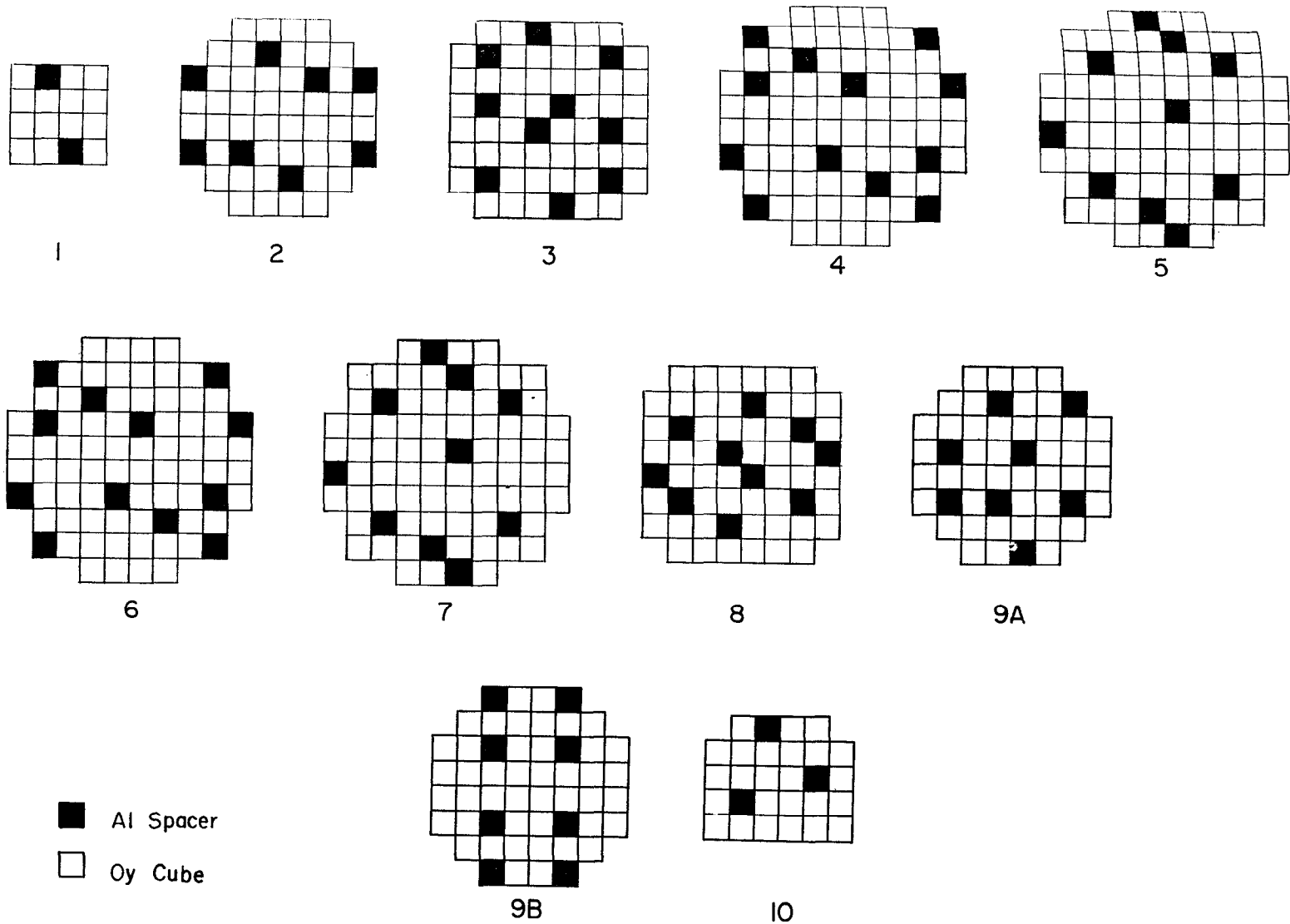
FIG. 7.   Stacking diagram for 5" pseudosphere; 85.4% density.

■ Al Spacer

☐ Oy Cube
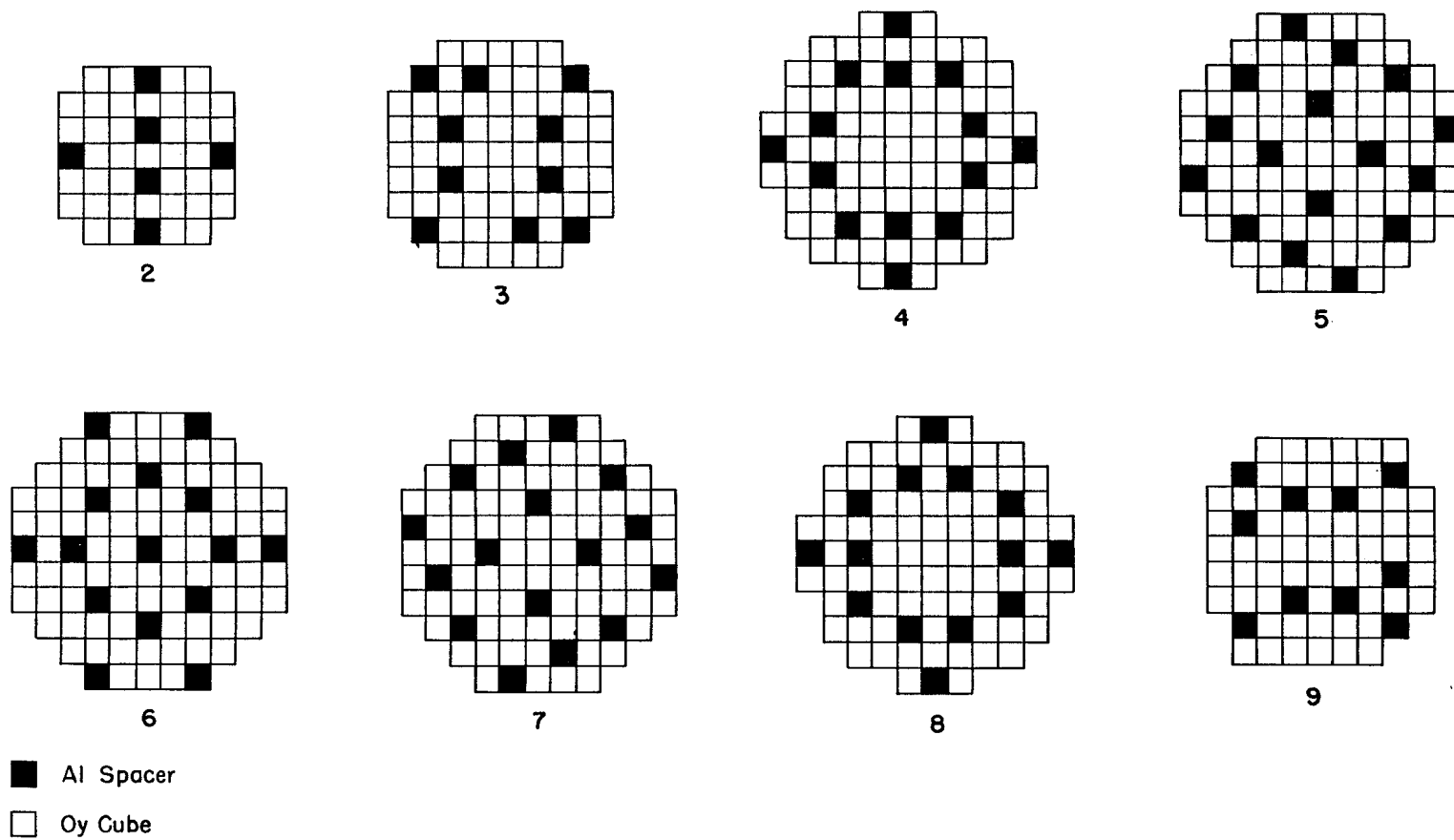
FIG. 8.   Stacking diagram for 5½" pseudosphere; 84.6% density.
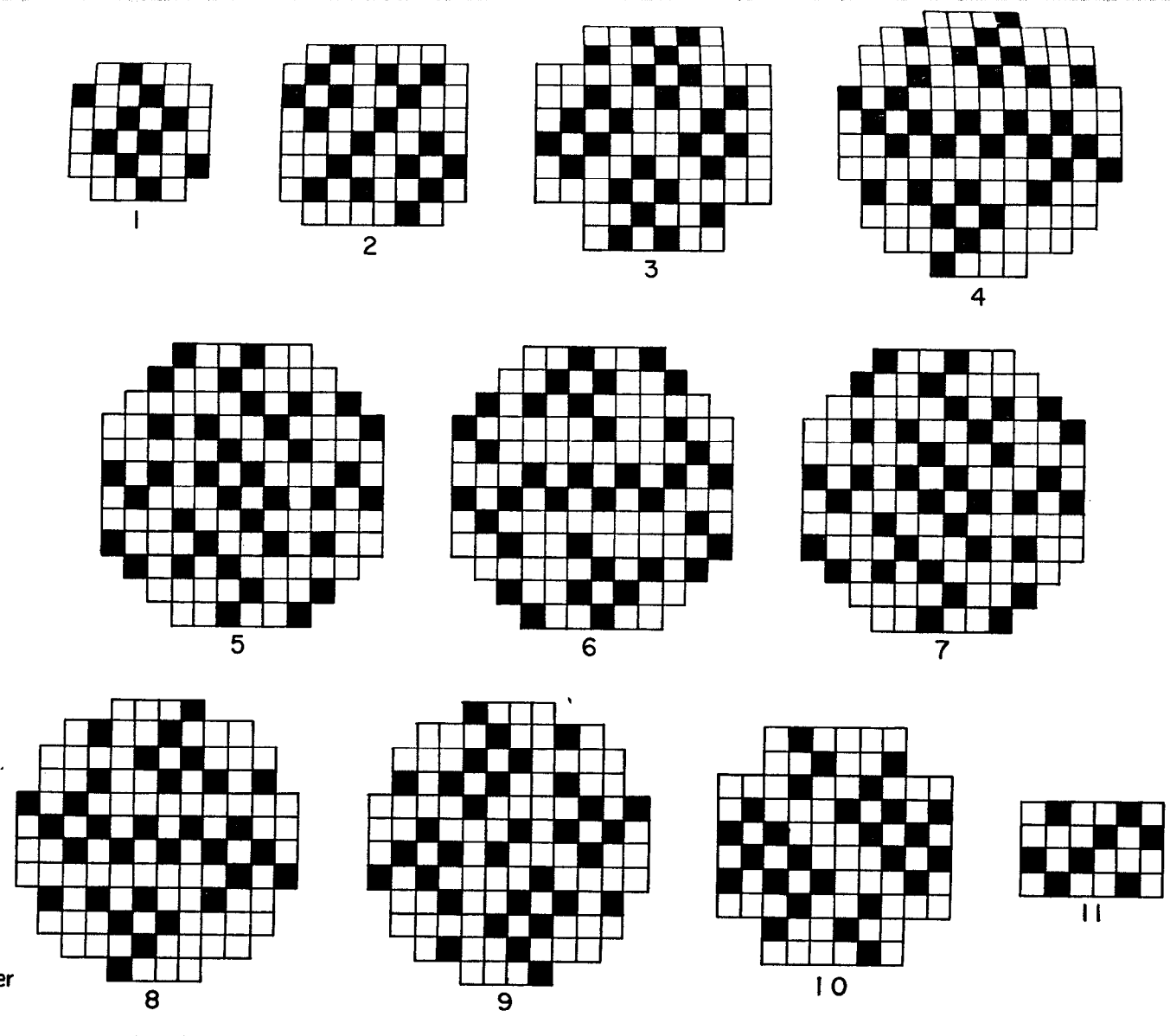
FIG. 9. Stacking diagram for 6" pseudosphere; 70.2% density.

■ Al Spacer
□ Oy Cube

■ Al Spacer
☐ Oy Cube
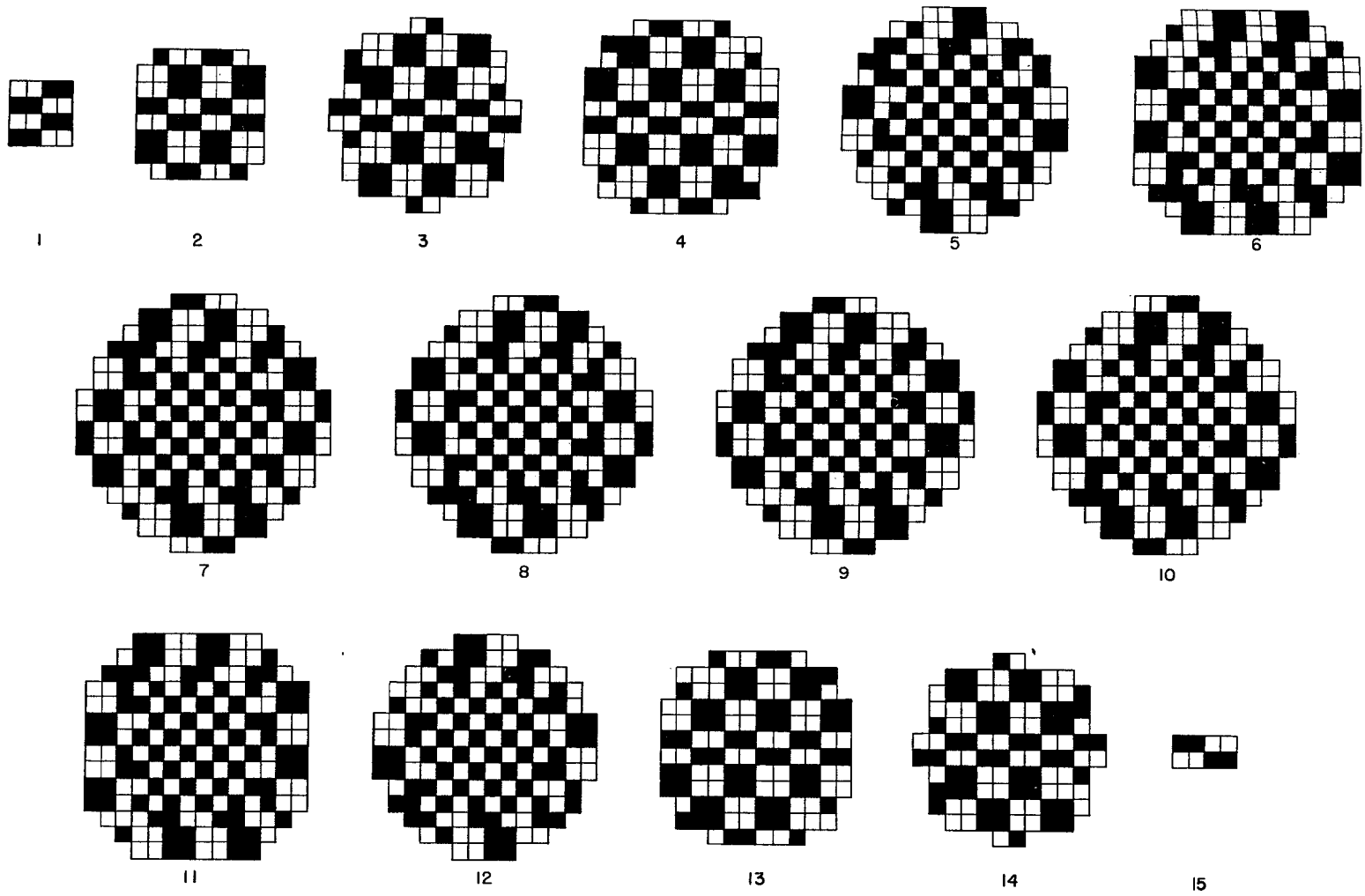
FIG. 10.   Stacking diagram for 8" pseudosphere; 50% density.

TABLE III. Critical mass vs core density for oralloy-tuballoy assembly.

Percent density	Pseudosphere size (in)	M_C with aluminum (kg)	Al Mass (gm)	M_C Corrected (kg)	No.units Oy	No.units Air	Density exponents
100	4.5			17.41	454		
85.4	5	20.82	157	20.93	543	93	1.17
84.6	5.5	21.21	160	21.34	553	101	1.22
70.2	6	26.58	480	26.93	693	294	1.23
70.2	6	26.23	963		684	290	
50.0	8	38.16	1484	39.34	995	995	1.18
50.0	8	37.05	2874		966	966	

D. Conclusion

The experimental measurements of low density and low concentration assemblies indicate that in the range from 50% to 100% of normal concentration and density the critical mass dependence on the oralloy core properties in the case of a thick tuballoy tamper is given by

$$M_c = \text{const } \rho^{-1.2} c^{-1.7}$$

The major objections to the method described here are 1) the use of finite units rather than a continuous distribution, and 2) the presence of rather large quantities of aluminum in some of the assemblies. For such a fast neutron assembly the mean free paths are large compared to the unit sizes, so very little perturbation should result from using ½ inch cubes. A check of the effect of cube size was made by the cube replacement technique in the case of the 50% density pseudosphere. The stacking diagram of Fig. 10 indicates that in the central region of the pseudosphere, oralloy units have aluminum neighbors on all six sides and aluminum spacers have nothing but oralloy neighbors. Substituting an oralloy cube for an aluminum spacer results in a serious disturbance of the stacking geometry. It was found, however, that the reactivity contribution of an oralloy cube in the aluminum position was equal to its reactivity contribution in the normal position.

No significant trend of the density exponent was observed with changing density. Similarly, the concentration exponent is constant within the experimental uncertainties of the measurements.

III.   REPLACEMENT TECHNIQUE FOR DERIVING THE
CONCENTRATION-DENSITY LAW

A.   Material Replacement Data

Critical mass vs density and concentration relation-
ships may be computed from contributions to reactivity by
small units of Oy and of Tu at various positions in the
Topsy Oy-Tu assembly. As described in detail in LAMS-1154,
data for such a computation are obtained from control rod
changes required to maintain the assembly at delayed criti-
cal when Oy or Tu is placed in a ½" cubic space. From a
control rod calibration curve, results are converted to
units of cents per mole[1]. In Table IV, reactivity con-
tributions of Oy and Tu are given as functions of radial
position in an Oy-Tu assembly of normal density (8½" thick
Tu tamper). Listed in Table V are data for a similar sys-
tem except that 50% normal Oy density is simulated in the
core (as described in Part II).

B.   Critical Mass vs Core Density

Let the reactivity contribution per mole of Oy (effec-
tive molecular weight M and density ρ) at the radius r be R(r).
Then the reactivity contribution per unit volume of Oy is $R\frac{\rho}{M}$
and the reactivity change per unit volume when ρ is changed by

---

[1] Control rod calibration methods and resulting curves are
described in LA-744 (Orndoff and Johnstone, 11/9/49).

TABLE IV. Material replacement data for the normal core density Topsy Oy-Tu assembly.

radius, r	Oy reactivity contribution R(r), cents/mole	$R(r)r^2$	Tu reactivity contribution $R_U(r)$, cents/mole	$R_U(r)r^2$
Data from split assembly, 6" can:				
0.50"	237.7	59.4	32.1	8.0
0.71"	230.8	116.4	33.1	16.7
1.12"	208.9	262.1	35.9	45.0
1.58"	176.0	439.5	39.7	99.1
2.06"	134.4	570.5	39.2	166.5
2.39" (interface)	102.2	585.0	30.5	174.7
2.55"	86.8	565.0	25.2	164.0
Data from solid ass'y, 8" can:[1]				
2.51"			27.8	175
2.56"			26.3	173
2.93"			14.8	127
3.54"			6.7	84
4.30"			2.8	52
4.71"			1.8	40
5.29"			0.9	25
5.58"			0.7	22

[1]Data for the 8" can was reduced 5% for best agreement with data for the 6" can in the neighborhood of the interface. This presumably corrects for a calibration discrepancy.

TABLE V. Material replacement data for the 50% core density Topsy Oy-Tu assembly.

radius, r	Oy reactivity contribution $R(r)$, cents/mole	Oy $R(r)r^2$	Tu reactivity contribution $R_U(r)$, cents/mole
0.374"	90.3	13	
1.273"	84.2	137	9.6
1.77"	78.8	247	
2.26"	72.3	369	9.9
2.76"	64.7	494	10.5
3.26"	56.8	604	10.5
3.76"	48.1	681	9.7
3.89" (interface)	46.1	699	9.3
4.14"	40.7	699	7.8

Note: Replacements in the core were made in lattice positions normally occupied by Oy. A few checks near the interface indicated that dependence on type of lattice position is within experimental error. The effect of possible increased differences nearer the core center is minimized by volume integration.

the small increment $\Delta\rho$ is $R\dfrac{\Delta\rho}{M}$. It follows that the reactivity change which results when the Oy density is changed by $\Delta\rho$ throughout the original core of critical radius r_o is

$$\Delta R = 4\pi \int_0^{r_o} R(r)\frac{\Delta\rho}{M}\, r^2 dr \ .$$

To maintain the system at delayed critical, the core volume must be changed by ΔV_c such that the reactivity change in interchanging Oy and Tu in ΔV_c equals ΔR. If for Tu (molecular weight M_U and density ρ_U) the reactivity change per mole at the core-tamper interface is $R_U(r_o)$, then this reactivity change may be expressed:

$$\Delta R \simeq \Delta V_c \left[R_U(r_o)\frac{\rho_U}{M_U} - R(r_o)\frac{\rho}{M} \right] \ , \quad \Delta\rho \ll \rho \ ;$$

so

$$4\pi \int_0^{r_o} R(r)\frac{\Delta\rho}{M} r^2 dr \simeq \Delta V_c \left[R_U(r_o)\frac{\rho_U}{M_U} - R(r_o)\frac{\rho}{M} \right] \ .$$

This may be combined with

$$\frac{\Delta M_c}{M_c} = \frac{\Delta V_c}{V_c} + \frac{\Delta\rho}{\rho} \ ,$$

the fractional change in critical mass, to give

$$\frac{\Delta M_c}{M_c} \simeq \frac{\Delta\rho}{\rho} \left\{ 1 + \frac{3\int_0^{r_o} R(r)r^2 dr}{r_o^3 \left[R_U(r_o)\frac{\rho_U M}{\rho M_U} - R(r_o) \right]} \right\} \cdot \quad (2)$$

Inserting $R(r_o) = 102.2$ cents/mole, $R_U(r_o) = 30.5$ cents/mole, $r_o = 2.39$ inches, and $\frac{\rho}{M} = \frac{\rho_U}{M_U}$, this expression becomes

$$\frac{\Delta M_c}{M_c} \simeq \frac{\Delta \rho}{\rho} \left[1 - 3.065 \times 10^{-3} \int_0^{r_o} R(r) r^2 dr \right] \quad,$$

and graphical integration of $R(r)r^2$ for Oy of normal density, represented in Fig. 11, gives

$$\frac{\Delta M_c}{M_c} \simeq -1.17 \frac{\Delta \rho}{\rho} \quad,$$

or

$$M_c \simeq const \; \rho^{-1.17} \quad. \tag{3}$$

The probable error in power of ρ is estimated as ± 0.03.

Although data for an Oy core of 50% normal density were obtained under less favorable conditions than for the core of full density, they provide an approximate check of the critical mass vs density relation of Part II. In this case, $R(r_o) = 46.1$ cents/mole, $R_U(r_o) = 9.3$ cents/mole, $r_o = 3.89"$, and $\frac{\rho}{M} = \frac{1}{2} \frac{\rho_U}{M_U}$, so (1) becomes

$$\frac{\Delta M_c}{M_c} \simeq \frac{\Delta \rho}{\rho} \left[1 - 1.85 \times 10^{-3} \int_0^{r_o} R(r) r^2 dr \right] \quad, \quad \Delta \rho \ll \rho$$

and another graphical integration (Fig. 12) gives

$$M_c \simeq const \; \rho^{-1.24} \quad. \tag{4}$$

Here the probable error in power of ρ may be ± 0.06.
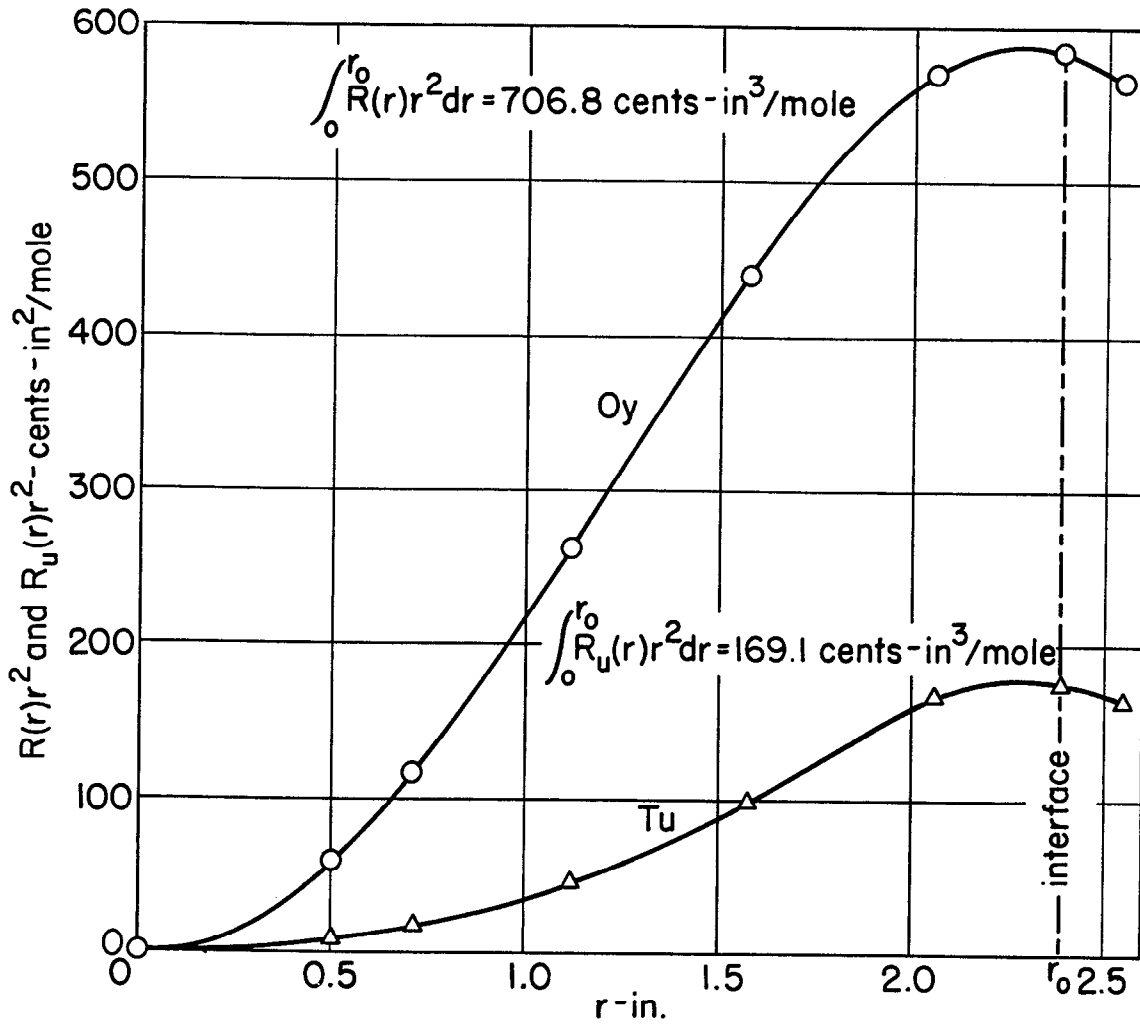
FIG. 11.   Functions to be integrated for M_C vs ρ and c in
the Topsy Oy-Tu assembly of normal density.
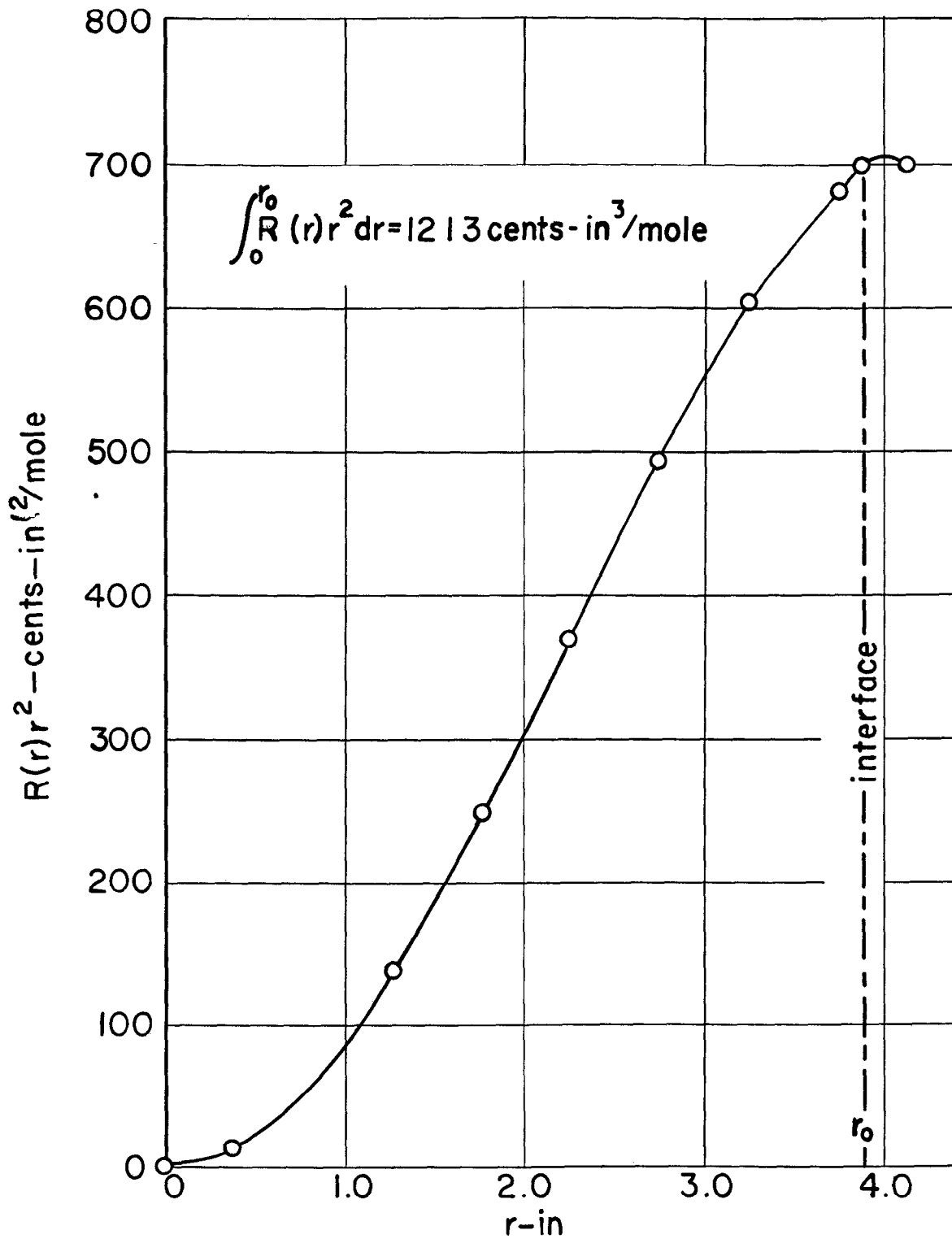
FIG. 12. Function to be integrated for M_C vs ρ in the Topsy Oy-Tu assembly with 50% density core.

The powers of (3) and (4) compare with the value -1.12 obtained from independent preliminary data on a full density Oy-Tu assembly and reported in LAMS-1154. These results are taken to confirm the more direct conclusions of Part II.

C. Critical Mass vs Tamper Density

The reactivity contribution figures for the Topsy configuration of normal density extend sufficiently into the tamper to permit an estimate of the relation between critical mass and tamper density. This is of interest because elementary general considerations lead to a relation of the form

$$M_c = \text{const } \rho(\text{core})^{-a}\rho(\text{tamper})^{-2+a} \quad ,$$

per Eq.(1) of Part I. For this case, the expression analogous to (2) is

$$\frac{\Delta M_c}{M_c} \simeq \frac{'\Delta \rho_U}{\rho_U} \; \frac{3 \int_{r_0}^{\infty} R_U(r)r^2 dr}{r_0^3 \left[R_U(r_0) - R(r_0)\frac{\rho M_U}{\rho_U M} \right]} \quad ,$$

since $\frac{\Delta \rho}{\rho} = 0$ and the tamper involved is effectively infinite. Parameters are the same as for the full Oy density case of the preceding section, so

$$\frac{\Delta M_c}{M_c} \simeq -3.065 \times 10^{-3} \left[\int_{r_0}^{\infty} R_U(r)r^2 dr \right] \frac{\Delta \rho_U}{\rho_U} \quad .$$

Graphical integration involves an extrapolation of $R_U(r)r^2$ to

a region of negligible contribution. The solid line of Fig. 13, a reasonable extrapolation, leads to

$$M_c \simeq \text{const } \rho_U^{-0.80} \, . \tag{5}$$

This is consistent with the low powers of ρ in (3), (4) and Part II.

As a check, recomputation for the extreme extrapolations represented by the dotted lines of Fig. 13 gives

$$M_c \simeq \text{const } \rho_U^{-0.80 \pm 0.034} \, .$$

Even these limits are inconsistent with the generally accepted $\rho^{-1.4}$ dependence of M_c.

D. Critical Mass vs Oy Concentration

A change in concentration of 25 in Oy (c to $c + \Delta c$) is equivalent to replacing U^{238} by U^{235} in the fraction Δc of each elementary core volume. Within experimental uncertainty, this is equivalent to replacing Tu by Oy in the fraction $\dfrac{\Delta c}{c}$ of the volume. Again, the reactivity change

$$\Delta R \simeq 4\pi \frac{\Delta c}{c} \int_0^{r_0} \left[R(r)\frac{\rho}{M} - R_U(r)\frac{\rho_U}{M_U} \right] r^2 dr$$

is compensated by the change in critical volume ΔV_c such that

$$\Delta R \simeq \Delta V_c \left[R_U(r_o)\frac{\rho_U}{M_U} - R(r_o)\frac{\rho}{M} \right] \, .$$

As $\dfrac{\rho_U}{M_U} = \dfrac{\rho}{M}$ and $\dfrac{\Delta M_c}{M_c} = \dfrac{\Delta V_c}{V_c}$ for normal ρ and ρ_U,

The graph shows a curve with the y-axis labeled $R_u(r)\,r^2$ - cents-in^2/mole ranging from 0 to 250, and the x-axis labeled r-in ranging from 2 to 10. A vertical dashed line labeled "interface" is at r_0. The equation displayed on the graph is:

$$\int_{r_0}^{\infty} R_u(r)\, r^2\, dr = 261.8 \text{ cents } -\text{in}^3/\text{mole}$$
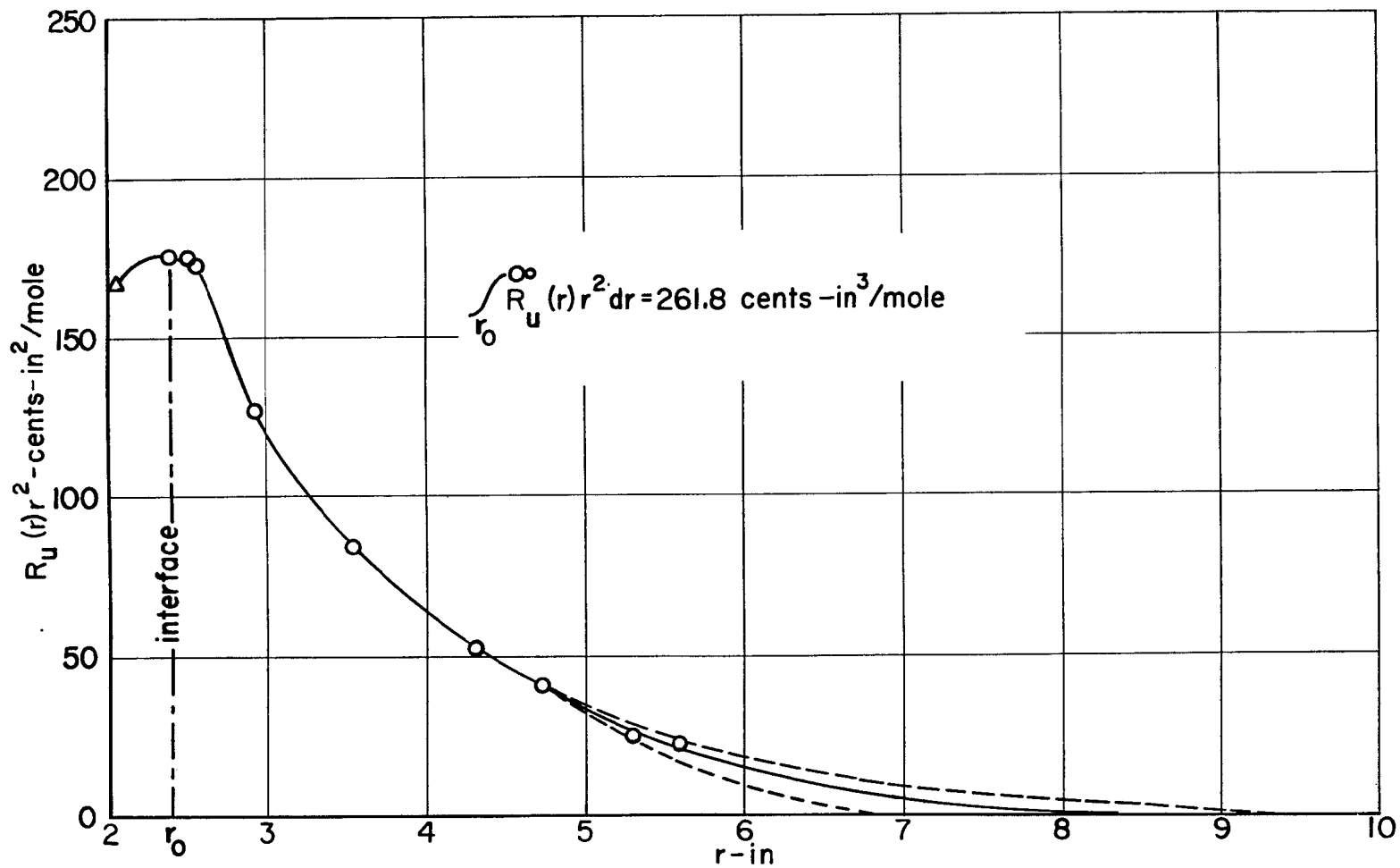
FIG. 13.   Function to be integrated for M_c vs ρ_U relation in the
Topsy Oy-Tu assembly of normal density.

$$\frac{\Delta M_c}{M_c} \simeq \frac{\Delta c}{c} \; \frac{3 \int_0^{r_0} \left[R(r) - R_U(r) \right] r^2 dr}{r_0^3 \left[R_U(r_0) - R(r_0) \right]} \qquad . \qquad (6)$$

$R_U(r_0) = 30.6$ and $R(r_0) = 102.2$ give

$$\frac{\Delta M_c}{M_c} \simeq -3.065 \times 10^{-3} \frac{\Delta c}{c} \int_0^{r_0} \left[R(r) - R_U(r) \right] r^2 dr .$$

Graphical integration per Fig. 11 leads to $M_c \simeq const \; c^{-1.65}$ (7) where a probable error of about ±0.03 should be assigned to the power of c. LAMS-1154 gives a power of -1.63 from independent preliminary data. The concentration relation (7), though not sufficiently well established for argument against the accepted $c^{-1.8}$ variation of critical mass, tends to support the conclusions of Part II.

Note: Recent material replacement measurements on an untamped subcritical assembly lead to the relation

$$M_c = const \; \rho^{-2.07 \pm 0.15} \qquad ,$$

where the expected power of ρ is -2.00. The corresponding concentration relation is

$$M_c = const \; \rho^{-1.78 \pm 0.15} \qquad .$$

Details are included in LA-1209 ("Measurements on Untamped Oralloy Assembly", Orndoff and Paxton, February 8, 1951).

Critical mass calculations utilize a limited number of material parameters related to the more basic cross sections by specific averages of the latter over the neutron energy spectra. Such calculations are sufficiently accurate to indicate a considerable discrepancy between the observed critical masses and the measured cross sections, and have resulted in the use of parameters empirically adjusted to give agreement with some set of critical mass data.

The aim of this section is to compare the observed critical radii of four Oy-Tu assemblies with the corresponding values computed using the recent Bethe-Weisskopf summary of neutron cross sections for Tu and Oy.[1] No attempt will be made to readjust the cross sections for better fitting to the data. The four assemblies are:

I.   Oy sphere, untamped;
$$M_c = 54.1 \text{ kg}^{(2)}$$

II. Oy sphere, tamped in infinite Tu;
$$M_c = 17.41 \text{ kg}$$

III. 50% density Oy sphere, tamped in infinite Tu;
$$M_c = 39.34 \text{ kg}$$

IV. 50% concentration Oy-Tu sphere; tamped in infinite Tu;
$$M_c = 57.23 \text{ kg}$$

---

[1] Memorandum from Richtmyer to Mark, Sept. 28, 1949.
[2] LA-1209, "Measurements on Untamped Oy Assembly".

A. Basis and Method of the Computations

Although the neutron energy spectra are different in the cores of each of these assemblies, the variation is small and will be characterized by a single parameter, γ, giving the ratio of neutron flux below 1 mev to that above 1 mev. (The number of energy groups into which the total flux should be divided depends mainly on the variation of the flux spectra in the different assemblies under consideration.)

The requisite set of two-group Oy and Tu cross sections is obtained with the aid of six-group flux spectra[3] (associated respectively with the flux in a bare Oy assembly and this flux modified by reflection from Tu) and the usual averaging scheme (see, for example, LA-53): a) transport cross sections as harmonic averages over the flux spectrum n_i, viz. $1/\sigma_t = \sum n_i/\sigma_{ti}$, and b) fission, absorption and inelastic scattering cross sections as direct averages over the flux. These values are listed in Table VI.

Two methods of calculation are used: $\underline{A}$) The two-group method given by Feynman and Welton in LA-524. For each assembly, except case I, two different results are given corresponding to the two "limiting" estimates of the return to the core of neutrons inelastically scattered in the tamper. $\underline{B}$) The method given by Serber in LA-234. For this calcula-

---

[3] Communicated by B. Carlson. (The cross sections from ref. 1 were used in the determination of these spectra.)

TABLE VI. Oy and Tu cross sections.

		Oy (barns)	Tu (barns)
Transport cross sections:	$\sigma_{t1}(>1 \text{ mev})$	4.217	4.135
	$\sigma_{t2}(<1 \text{ mev})$	6.639	6.176
Fission cross sections:	σ_{f1}	1.246	0.325
	σ_{f2}	1.437	0.011
Capture cross sections:	σ_{a1}	0.005	0.064
	σ_{a2}	0.076	0.162
Inelastic scattering cross sections:	σ_{12}	1.10	1.56
		Oy	Tu
Fission spectrum	χ_1	.67	.67
	χ_2	.33	.33
Neuts per fission	ν	2.5	2.5

tion, a value of γ obtained in Method A permits the determination of an appropriate set of one-group core cross sections. The tamper reflection for cases II-IV is computed using the two-group asymptotic flux distributions, the spectrum being matched to γ at the tamper-core interface. (The neutron spectrum in the tamper, unlike the core, is strongly dependent upon radial position, and in this sense one-group tamper cross sections are rather artificial. Nevertheless, Table VII includes a listing of the reproduction numbers, f', giving the proper tamper reflection when the transport cross section is arbitrarily assigned at 6.0 barns. The near constancy of the values indicates that a single pair of f', σ_t' numbers would serve quite well for all of the three assemblies.) Method B is to be preferred as it is not burdened with the approximations required for the simultaneous furnishing of a neutron energy spectrum, and as it also utilizes a graphical evaluation scheme which has been altered slightly from the predictions of the Serber theory so as to give agreement with more exact calculations at the few points where such are available (see LA-234 for details).

B. Comparison of the Observed and Computed Critical Radii

The direction of the discrepancy between computed and observed critical assemblies has led to the suspicion (ex-

TABLE VII.

1. Critical radii and γ (core flux <1 mev / core flux >1 mev) computed by Method A.

Assembly	"upper limit"	"lower limit"	γ
I	8.27 cm	8.27 cm	1.01
II	5.90 cm	5.74 cm	1.33
III	9.89 cm	9.64 cm	1.58
IV	8.99 cm	8.69 cm	2.06

2. Computed critical radii and associated one-group cross sections ala Method B and the corresponding observed critical radii.

Assembly	Computed	Observed
I	($\sigma = 5.162$b.; $f = .382$) $r_1 = 8.35_1$ cm	$r_1 = 8.87_1$ cm
II	($\sigma = 5.326$b.; $f = .373$) ($\sigma' = 6.0$ b.; $f' = -.0155$) $r_2 = 5.69_4$ cm $r_2/r_1 = .682$	$r_2 = 6.05_5$ cm $r_2/r_1 = .683$
III	($\sigma = 5.429$b.; $f = .368$) ($\sigma' = 6.0$ b.; $f' = -.0145$) $r_3 = 9.44_8$ cm $r_3/r_1 = 1.131$	$r_3 = 10.01$ cm $r_3/r_1 = 1.128$
IV	($\sigma = 5.456$b.; $f = .188$) ($\sigma' = 6.0$ b.; $f' = -.0156$) $r_4 = 8.61_1$ cm $r_4/r_1 = 1.031$	$r_4 = 8.99_4$ cm $r_4/r_1 = 1.014$

pressed by Bethe, Barschall and others) that the directly

measured cross sections are too large. Thus the particular

feature that the computed critical radius is less than the

observed in each of the four present cases was to be expect-

ed. Since the scaling down of all cross sections leaves un-

altered the ratios of computed radii (and hence, of course,

the predicted concentration and density exponents), it is of

interest to note how well these agree with the observed ra-

tios. From Table VII it is seen that the first three cases

are consistent with a simple scaling down of the cross sec-

tions, and thus also that the computed density exponent is

-1.20 in the 50-100% normal density range. The computed re-

lative radius of the 50% concentration assembly, however, is

$\sim 1\frac{1}{2}\%$ too large and gives a concentration exponent of -1.79

as compared to the experimental value of -1.73. Although

this disagreement cannot be attributed unambiguously to any

one cross section, it is nevertheless true that using a re-

latively larger "28" fission cross section would improve the

computed concentration exponent without much damage to the

present good agreement in the other cases.

Further information on assemblies I-III is available

in the form of comparative activations of Oy and "28" pieces

(see W-2 Progress Reports for May-June 1950; Sept.-Oct. 1950

and Nov.-Dec. 1950). The ratio, R, of Oy to "28" activation

is related to the two-group flux ratio, γ, by the equation

$$\gamma = \frac{\dfrac{\sigma_{f1}(28)}{\sigma_{f1}(Oy)} R - 1}{\sigma_{f2}(Oy) / \sigma_{f1}(Oy)} \quad .$$

Figure 14 gives R as a function of radius for assemblies II and III and indicates the nearly constant spectrum through the core and the rapidly changing spectrum in the tamper. The average core γ's as obtained from the Oy-"28" activation ratio and those obtained from the Feynman method are summarized below.

TABLE VIII

Assembly	R	γ(R)	γ(Meth.A)
I	6.1	.51 (.71)	1.01
II	8.7	1.10 (1.38)	1.33
III	9.0	1.16 (1.46)	1.58

The values of γ contained in parentheses arise in the following way: In obtaining the two-group cross sections from the work of Ref. 3, the tuballoy cross sections were determined using a spectrum characteristic of neutrons returning from the tamper. This spectrum has a γ value of 1.91, which is somewhat higher than the values for the cores in which the "28" foils were used. Although the two-group Oy cross sections are quite insensitive to the variation of spectra encountered in the above four assemblies, the "28" fission cross
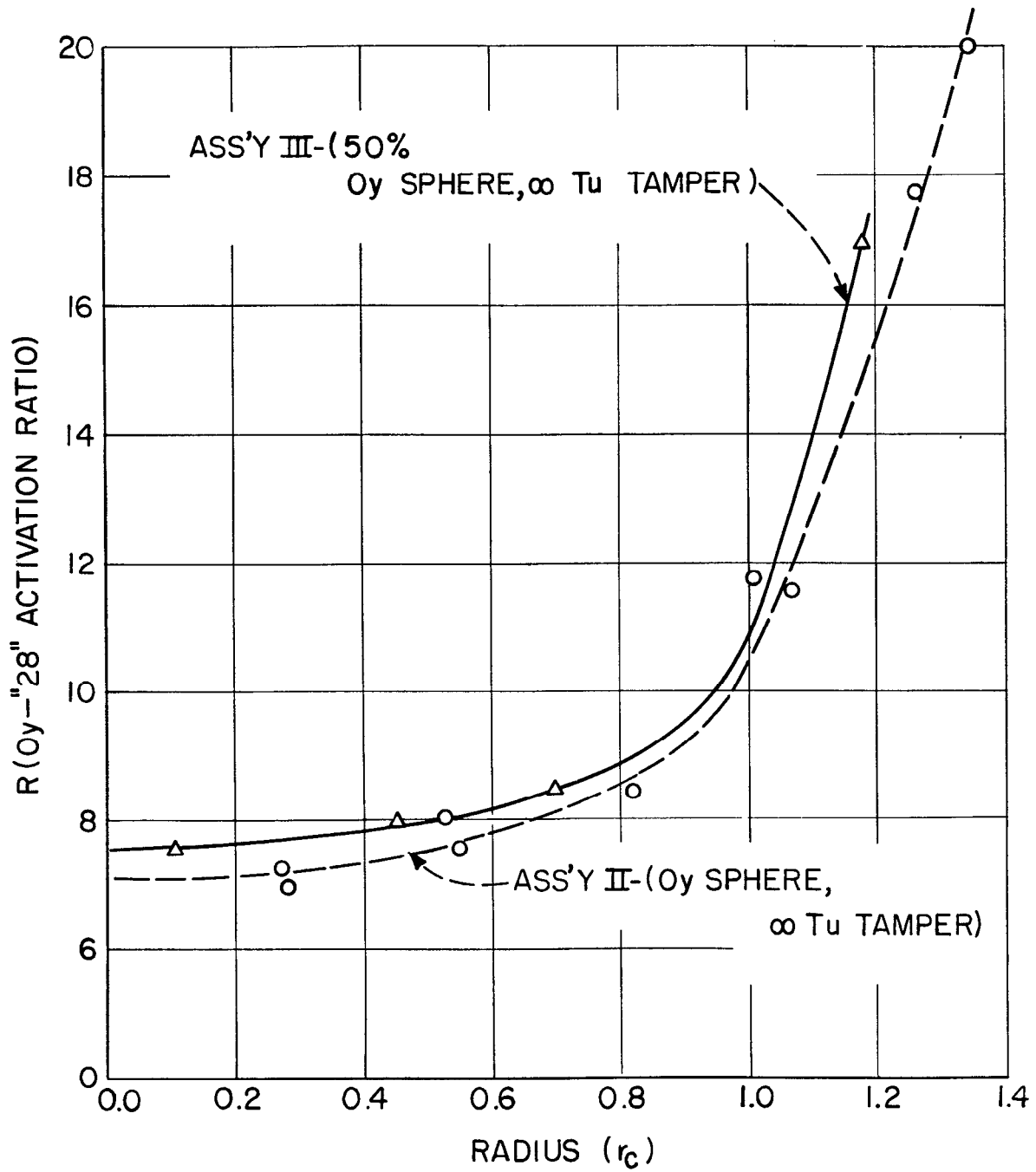
FIG. 14. Ratio of activation of Oy and "28" foils as a function of radius for Assemblies II and III.

section is not, and if determined by averaging over the six-group Oy spectrum given in Ref. 3 ($\gamma = 1.06$), then $\sigma_{f1}(Tu) = .375$ barns as compared to .325 barns given in Table VI and used in the computations of critical radii. The values of $\gamma(R)$ in parentheses are obtained using this larger value of $\sigma_{f1}(Tu)$ and thus represent upper limits. The general inequality $\gamma(R) < \gamma$ (Meth. A) evident from Table VIII also indicates that the measured fission cross section of "28" is relatively too small (it is to be admitted that as a whole the absolute values of Oy and Tu cross sections are too large) under the plausible assumption that Method A gives the more accurate value for γ.

C. Qualitative Remarks on the Density Exponent

In both the limit of very high and very low core densities (high or low relative to the tamper density), the density exponent is -2. This follows in the high density case because the core radius is small compared to the neutron mean free path in the tamper, and the assembly is thus in the limit equivalent to the untamped core where of course the density exponent is -2. In the low density case, the radius of the core is large compared to the neutron mean free path in the tamper. Thus the surface of the core appears as a plane to neutrons in the tamper. The net escape of core neutrons is then propor-

- 45 -

tional to the core surface whereas the production is proportional to the volume and to the number of fissionable nuclei per unit volume; i.e. $r^2 \propto \rho r^3$ and $M_c \propto \rho^{-2}$. In the intermediate density range, the magnitude of the exponent is less than two and assumes a broad minimum in the vicinity of 50-100% normal core density. The critical mass vs density measurements presented above constitute then a determination of this minimum value.

D.   Qualitative Remarks on the Concentration Exponent

The critical infinite uranium assembly occurs at a finite "25" concentration, and at this point the concentration exponent is $-\infty$. A plausibility argument, somewhat on the marginal side, as to the observed constancy of the exponent in the 50-100% range is as follows. In the initial stages of diluting "25" with "28", capture cross sections are relatively unimportant, the primary effect being a reduction of the fission cross section per nucleus and thus a shifting towards the diffusion limit $(\nu - 1)\sigma_f \ll \sigma_t$ where the critical radius behaves as $(\sigma_f \sigma_t)^{1/2} r_c \simeq$ const. Very nearly $\sigma_f = c\sigma_{fo}$ where c is the "25" concentration and σ_{fo} the "25" fission cross section. Thus the initial shift is towards the limit $c^{1/2} r_c \simeq$ const. or $M_c \propto c^{-1.5}$. It is this effect in competition with the increasing absorption which tends to maintain the

concentration exponent at -1.71 in the high concentration range.

Summary

The observed critical radii of the four Oy-Tu assemblies again support the suspicion that the experimental cross sections are too high. The critical radii of the untamped Oy sphere and the Tu tamped, low density Oy spheres are consistent with the simple scaling down of the Bethe-Weisskopf cross sections by about 5%. However, for the low concentration assemblies, this type of cross section readjustment is insufficient as shown by the incorrect prediction of the concentration exponent. This is likely associated with the "28" fission cross section which appears relatively too low, an appearance, however, that may well be due to an inadequacy of the method of calculation. For the untamped assembly, the concentration exponent value $-1.78\pm.15$, determined from reactivity measurements, compares favorably with the calculated value -1.81 (using two-group Tu cross sections obtained by averaging over the Oy spectrum).